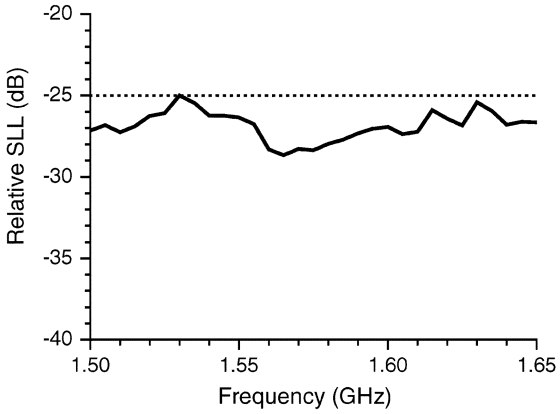

Fig. 6. Measured relative SLL versus the frequency.

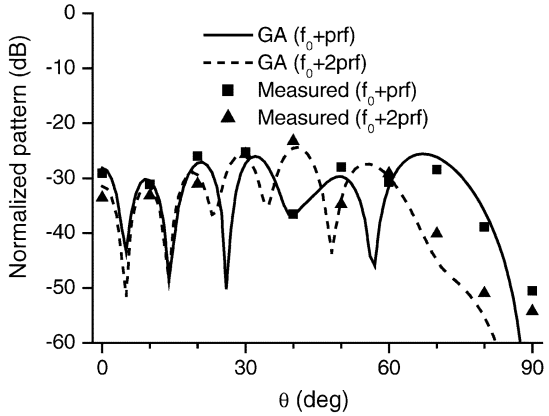

Fig. 7. Measured sideband patterns in comparison with the theoretical patterns.

which is in good agreement with the theoretical SLL of -25.5 dB. Fig. 6 plots the measured relative SLL versus frequency from 1.50 to 1.65 GHz. The SLLs are below -25 dB across the operation frequency band. The first two sideband patterns were also measured using a spectrum analyzer at different angles. In this case, the large reflector antenna in the compact range was used to transmit a CW signal at 1.56 GHz, and a spectrum analyzer outside the compact range was directly connected to the output of the time modulated linear array. The measured relative sideband patterns at the first two sideband frequencies $f_0 + prf, f_0 + 2prf$ are shown in Fig. 7 in comparison with those of the GA optimized results. It is observed that the measured sideband patterns are in reasonable agreement with those of the GA optimized patterns, especially near the bore sight region. The measured SBL is about -23.3 dB, which is close to the GA optimized value of -24.6 dB.

V. Conclusion

This paper describes a time modulated linear arrays with uniform amplitude, low SLL and low SBL simultaneously. The time modulation period was divided into minimal time steps, and the ON-OFF status for each of these minimal time steps was optimized directly via a SGA on each array element. Based on the numerical results, the SLL and SBL can be simultaneously suppressed to below -25 dB for a 16-element time modulated linear array. An *L*-band 16-element printed dipole linear array with its associated feed network for time modulation was developed, and the GA optimized time sequences were implemented in the feed network. Measured results are in good agreement with the simulation results, thereby confirming the proposed method.

References

[1] R. W. Bickmore, "Time versus space in antenna theory," in *Microwave Scanning Antennas*, R. C. Hansen, Ed. New York, NY: Academic, 1966, vol. III.

[2] W. H. Kummer, A. T. Villeneuve, T. S. Fong, and F. G. Terrio, "Ultra-low sidelobes from time-modulated arrays," *IEEE Trans. Antennas Propag.*, vol. AP-11, no. 6, pp. 633–639, Nov. 1963.

[3] B. L. Lewis and J. B. Evins, "A new technique for reducing radar response to signals entering antenna sidelobes," *IEEE Trans. Antennas Propaga*, vol. 31, no. 6, pp. 993–996, Nov. 1983.

[4] S. Yang, Y. B. Gan, and A. Qing, "Sideband suppression in time-modulated linear arrays by the differential evolution algorithm," *IEEE Antennas Wireless Propagat. Lett.*, vol. 1, pp. 173–175, 2002.

[5] S. Yang, Y. B. Gan, and P. K. Tan, "A new technique for power-pattern synthesis in time-modulated linear arrays," *IEEE Antennas Wireless Propagat. Lett.*, vol. 2, pp. 285–287, 2003.

[6] ——, "Evaluation of directivity and gain for time modulated linear antenna arrays," *Microwave Opt. Tech. Lett.*, vol. 42, no. 2, pp. 167–171, July 2004.

[7] ——, "Comparative study of low sidelobe time modulated linear arrays with different time schemes," *J. Electromagn. Waves Appl.*, vol. 18, no. 11, pp. 1443–1458, Nov. 2004.

[8] D. G. Kurup, M. Himdi, and A. Rydberg, "Synthesis of uniform amplitude unequally spaced antenna arrays using the differential evolution algorithm," *IEEE Trans. Antennas Propag.*, vol. 51, no. 9, pp. 2210–2217, Sep. 2003.

[9] Y. Rahmat-Samii and E. Michielssen, *Electromagnetic Optimization by Genetic Algorithms*. New York: Wiley, 1999.

A Generalized Sidelobe Canceller Employing Two-Dimensional Frequency Invariant Filters

Wei Liu, Stephan Weiss, and Lajos Hanzo

***Abstract*—Based on the generalized sidelobe canceller (GSC), we propose a novel adaptive broadband beamformer, where the quiescent vector and blocking matrix are replaced by a series of two-dimensional frequency invariant filters (FIFs). As opposed to standard beamspace techniques, the number of FIFs is flexible and they are not required to posses a very low sidelobe level. Compared with a standard GSC, a faster convergence speed and a lower computational complexity of its adaptive part are achieved.**

***Index Terms*—Adaptive broadband beamforming, frequency invariant beamforming, generalized sidelobe canceller, two-dimensional (2-D) filters.**

I. Introduction

Adaptive beamforming has found numerous applications in various areas ranging from sonar and radar to wireless communications [1]. For arrays to accomplish nulling over a wide bandwidth, tapped-delay lines (TDLs) are employed, resulting in a beamformer with M sensors and TDLs of length J, as shown in Fig. 1. To perform beamforming

Manuscript received August 7, 2003; revised September 24, 2004.

W. Liu is with the Communications and Signal Processing Research Group, Department of Electrical and Electronic Engineering, Imperial College London, SW7 2BT, U.K. (e-mail: wei.liu@imperial.ac.uk).

S. Weiss and L. Hanzo are with the Communications Research Group, School of Electronics and Computer Science, University of Southampton, SO17 1BJ, U.K. (e-mail: s.weiss@ecs.soton.ac.uk; l.hanzo@ecs.soton.ac.uk).

Digital Object Identifier 10.1109/TAP.2005.850759

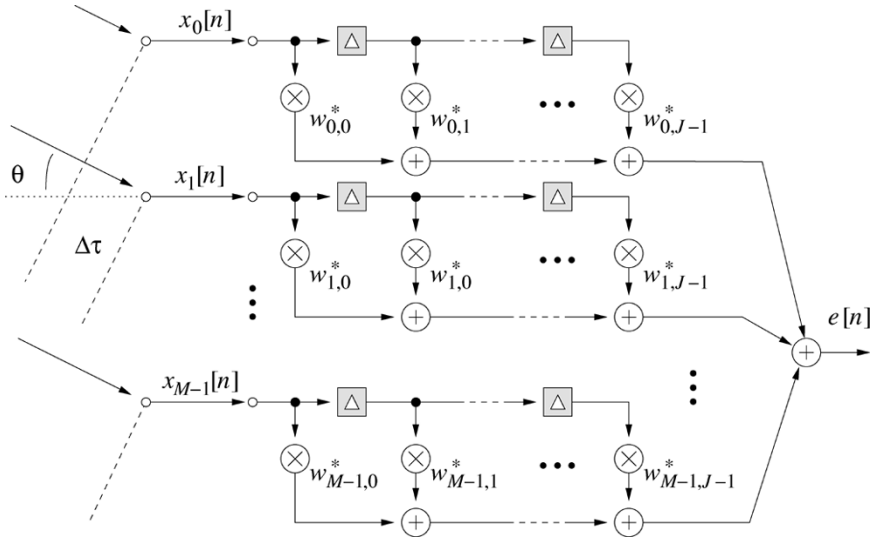

Fig. 1. A signal impinges from an angle θ onto a uniformly spaced broadband linear array with M sensors, each followed by a J-tap filter.

with high interference rejection and resolution, we need to employ a large number of sensors and long TDLs, which unavoidably increases the computational complexity of its adaptive part and slows down the convergence of the system. To overcome this problem, several methods have been proposed, such as the use of adaptive pole-zero filters in [2], subband adaptive methods in the temporal domain in [3] and [4] or both the temporal and spatial domains in [5]. Another method is the broadband beamspace adaptive array [6], where several frequency invariant beams are formed pointing to different directions by a fixed beamforming network with two-dimensional (2-D) filters; thereafter an adaptive filter is used to combine these beam outputs to form the desired output. Since both the number of beams and the number of selected beams are small, the total number of adaptive weights is greatly reduced.

In this paper, we apply the broadband beamspace technique to the generalized sidelobe canceller (GSC) structure [7], and propose a novel broadband adaptive beamformer, where the quiescent vector and the column vectors of the blocking matrix are replaced by a series of 2-D frequency invariant filters (FIFs). A beam pointing toward the signal of interest takes the role of the quiescent vector, whereas the blocking matrix is formed by a number of beams covering the remaining space, with a zero response formed toward the signal of interest. A design of such a quiescent vector and blocking matrix is also provided, based on the fan filter method proposed in [6].

In Section II, we will first give a brief review of the GSC structure and the frequency invariant beamforming technique based on fan filters and then propose the GSC with 2-D FIFs. The design of the blocking matrix FIFs is described in Section III. Simulation results are given in Section IV and conclusions drawn in Section V.

II. GSC Employing 2-D FIFs

A. GSC

A linearly constrained minimum variance (LCMV) beamformer [8] performs the minimization of the output signal's variance with respect to some given spatial and spectral constraints. The LCMV problem can be formulated as

$$\min_{\mathbf{w}} \mathbf{w}^{\mathrm{H}} \mathbf{R}_{xx} \mathbf{w} \quad \text{subject to} \quad \mathbf{C}^{\mathrm{H}} \mathbf{w} = \mathbf{f} \tag{1}$$

where $\mathbf{R}_{xx}$ is the covariance matrix of the received signal $\mathbf{x} = [x_0[n] x_1[n] \cdots x_{M-1}[n]]$, $\mathbf{w}$ is the weight vector, $\mathbf{C} \in \mathbb{C}^{MJ \times J}$ is the constraint matrix and $\mathbf{f}$ is the response vector.

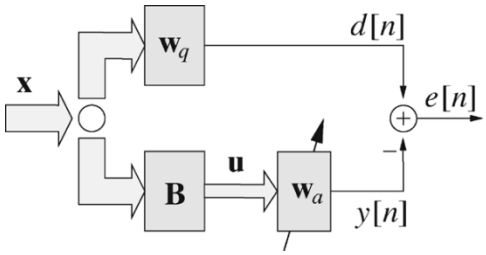

Fig. 2. GSC structure.

The constrained optimization of the LCMV problem in (1) can be conveniently solved using a GSC as shown in Fig. 2. The GSC performs a projection of the data onto an unconstrained subspace by means of a blocking matrix $\mathbf{B}$ and a quiescent vector $\mathbf{w}_q$. Thereafter, standard unconstrained optimization algorithms such as the least mean square (LMS) or recursive least squares (RLS) algorithms may be invoked [9].

Since $\mathbf{w}_q$ is designed to satisfy the specified constraints, the signal of interest will pass through the beamformer having a desired response independent of $\mathbf{w}_a$. In the lower branch, the blocking matrix is required to block the signal of interest so that only interfering signals and noise exist. When adapting $\mathbf{w}_a$, the scheme will tend to cancel the interference and noise component from $d[n]$, while minimizing the variance of the output signal $e[n]$.

Next, we will review the frequency invariant beamforming technique based on fan filters and then propose a new construction of the quiescent vector and the blocking matrix.

B. GSC Employing 2-D Frequency Invariant Filters

The response of the uniformly spaced linear array shown in Fig. 1 to a signal with an angular frequency ω and an angle of arrival θ can be written as [10]

$$\tilde{R}(\omega, \theta) = \sum_{m=0}^{M-1} \sum_{k=0}^{J-1} w^*_{m,k} \cdot e^{-jm\omega\Delta\tau} \cdot e^{-jk\omega T_s}$$

$$\text{with} \quad \Delta\tau = \frac{d}{c} \sin\theta \tag{2}$$

where T_s is the temporal sampling period and c is the wave propagation speed. Using the normalized angular frequency $\Omega = \omega T_s$, we obtain the response as a function of Ω and θ

$$R(\Omega, \theta) = \sum_{m=0}^{M-1} \sum_{k=0}^{J-1} w^*_{m,k} \cdot e^{-jm\mu\Omega\sin\theta} \cdot e^{-jk\Omega} \text{ with } \mu = \frac{d}{cT_s}. \tag{3}$$

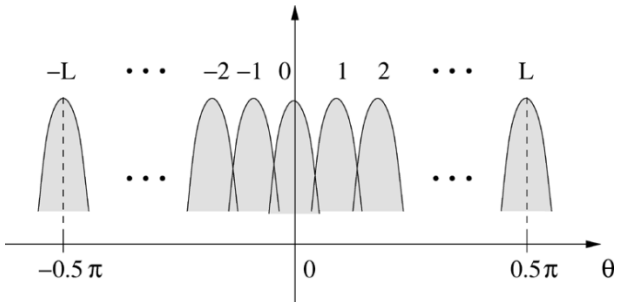

Fig. 3. An arrangement of the $2L+1$ main beams, which point to the directions $\theta_l = l\pi/2L, l = -L, \cdots, 0, \cdots, L$.

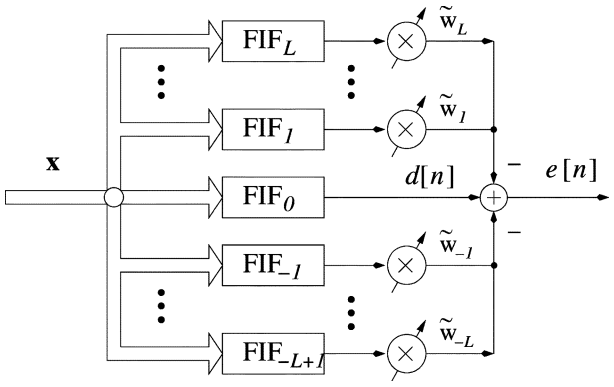

Fig. 4. GSC consisting of the proposed FIFs.

With the substitution of $\Omega_1 = \Omega$ and $\Omega_2 = \mu\Omega\sin\theta$ in (3), we obtain a 2-D digital filter response

$$R(\Omega_1, \Omega_2) = \sum_{m=0}^{M-1}\sum_{k=0}^{J-1} w_{m,k}^{*} \cdot e^{-jk\Omega_1} \cdot e^{-jm\Omega_2}. \tag{4}$$

As the spatio-temporal spectrum of the received signal lies on the line $\Omega_2 = \mu\Omega_1\sin\theta$, we can use the transformation $\tilde{\Omega} = ((\Omega_2/\mu\Omega_1) - \sin\theta)\cdot\pi$ to obtain the coefficients $w_{m,k}^{*}$ from a one-dimensional (1-D) filter $H(e^{j\tilde{\Omega}})$. The resultant beamformer will have a frequency invariant response [6]. If $H(e^{j\tilde{\Omega}})$ is a low-pass filter [6], then signals from the directions around θ will correspond to its passband. In this case, a main beam is formed pointing to the direction θ.

When applying this broadband beamforming technique to the GSC, we replace $\mathbf{w}_q$ by a 2-D FIF with its main beam pointing to the signal of interest. For the blocking matrix, each column vector is replaced by a 2-D FIF having a zero response to the signal of interest. By this arrangement, the broadband beamforming problem is transformed into a narrowband beamforming problem. If the filters are strictly frequency invariant, then we only need $M-1$ such filters in the blocking matrix and only a single adaptive weight is required at each filter output. Thus, the total number of adaptive weights is reduced significantly.

Without loss of generality, assuming that the signal of interest comes from broadside, the main beam of $\mathbf{w}_q$ should point to the direction of $\theta = 0$. The blocking matrix is arranged such that its column vectors form L FIFs with their main beam directions equally distributed over $\theta \in [-(\pi/2); 0)$ and the same number over $\theta \in (0; (\pi/2)]$. Note that the Lth FIF and $-L$th FIF actually point to the same direction, therefore we only need one of them and there are in total $2L-1$ FIFs in the blocking matrix. All of the $2L-1$ FIFs should have a zero response at $\theta = 0$. Fig. 3 shows the arrangement of the $2L+1$ main beams, which point to the directions $\theta_l = l\pi/2L$, $l = -L, \cdots, 0, \cdots, L$, respectively. A GSC based on these FIFs is shown in Fig. 4, where the FIF with index 0 implements the quiescent vector and the remaining FIFs form the blocking matrix. If the $2L-1$ FIFs in the blocking matrix are strictly frequency invariant, $2L-1$ should be equal to $M-1$. Here we set $L = \lceil (M-1)/2 \rceil$, where $\lceil\cdot\rceil$ is the ceiling (or round-up) operator.

As mentioned, the FIF in the proposed method transforms the broadband beamforming problem into a narrowband beamforming problem. As long as the FIFs have a good frequency invariant property, it is not necessary for them to have a very low sidelobe level, which is different from the condition on the FIFs in the beamspace processing method [6], where a low sidelobe level is required, resulting in a large dimension of the FIFs and the requirement to increase the number of sensors. Moreover, in [6], the main direction of a beam should ideally coincide with nulls (zero responses) of all other beams. As a result, the interference cancellation capability is reduced compared to the traditional GSC method. As an example, consider the case of a five-tap prototype FIR filter. Since this prototype has only four zeros, the maximum number of frequency invariant beams achieved in the beamspace method is five, as shown in [6]. According to [6], to attain a good frequency invariant characteristic, the values of M and J have to be at least three times the length of the prototype filter, i.e., $M, J \geq 15$ for the five-tap prototype FIR filter. Comparing the number of beams, which is 5, with the number of antennas $M \geq 15$, we may have sacrificed an excessive degree of freedom of the system and hence a decreased performance is likely to result in some circumstances. However, in our proposed method, the FIFs in the blocking matrix only need to have a single zero in the direction of the signal of interest, so that it is possible to implement a large number of FIFs—in our case $(2L-1)$—even for a relatively small number of antenna elements M. A new design will be described in the next section to overcome the limitation of the beamspace method. Thus, by our approach, most of the interference cancellation capability of the array is retained. As a comparison, the number of FIFs, N_{FIF}, achieved for the beam space method and our proposed method compares as

$$N_{\mathrm{FIF}} \approx \begin{cases} \leq \frac{M}{3}, & \text{for beam space method} \\ 2\cdot\left\lceil \frac{M-1}{2} \right\rceil, & \text{for the proposed method.} \end{cases} \tag{5}$$

III. Design of the Frequency Invariant Filters

Since the FIF in $\mathbf{w}_q$ is a classic 2-D FIF pointing to the direction of the signal of interest θ_s without any imposed zeros, it can be directly obtained using the method of [6]. To design FIFs with appropriately imposed zeros for the blocking matrix, in the following, we present a 2-D filter design approach, which is a modified version of the approach proposed in [6].

Suppose $h[k]$ is a P-tap low-pass FIR filter having a frequency response $H(e^{j\tilde{\Omega}})$. Our aim is to derive the 2-D FIF from it with a main beam in the direction θ_i and a zero response formed toward the direction θ_s. Using the transformation $\tilde{\Omega} = ((\Omega_2/\mu\Omega_1) - \sin\theta_i)\cdot\pi$, we obtain the frequency response $R(\Omega_1, \Omega_2)$

$$R(\Omega_1, \Omega_2) = H\left(e^{j\left(\frac{\Omega_2}{\mu\Omega_1} - \sin\theta_i\right)\cdot\pi}\right). \tag{6}$$

As $R(\Omega_1, \Omega_2)|_{\theta=\theta_s} = 0$ and $\Omega_2/\mu\Omega_1 = \sin\theta_s$ in the direction $\theta = \theta_s$, we obtain

$$R(\Omega_1, \Omega_2)|_{\theta=\theta_s} = H\left(e^{j(\sin\theta_s - \sin\theta_i)\cdot\pi}\right) = 0. \tag{7}$$

Thus, the prototype filter design for the FIFs can be formulated as

$$h[k] = \arg\min_{h[k]} \Phi_l \quad \text{subject to} \quad (7) \tag{8}$$

where

$$\Phi_l = \int_{\tilde{\Omega}_s}^{\pi} \left|H(e^{j\tilde{\Omega}})\right|^2 d\tilde{\Omega} \tag{9}$$

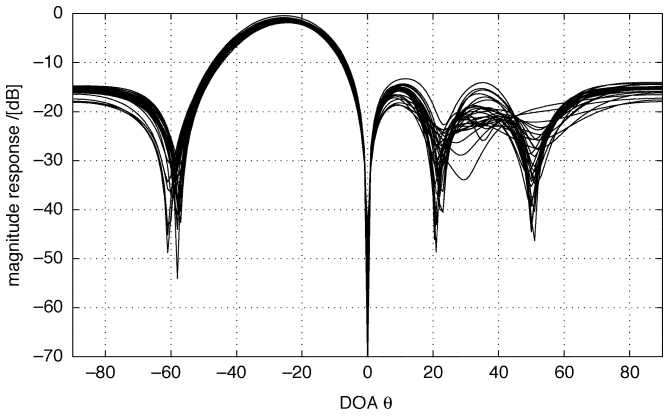

Fig. 5. Magnitude response of an FIF example over the band $\Omega \in [0.35\pi; 0.95\pi]$ with its main beam pointing to $\theta_i = -25^\circ$.

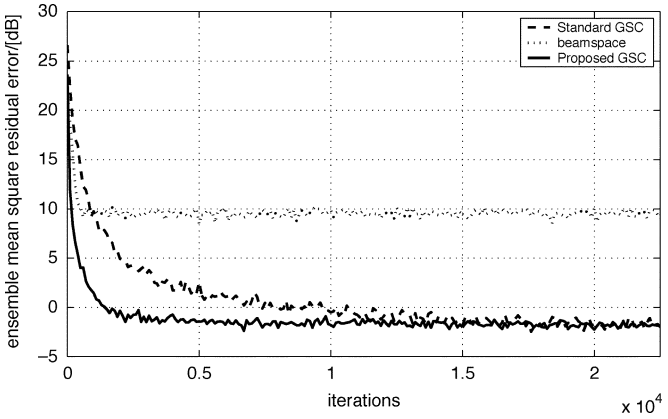

Fig. 6. Learning curves for different methods.

is the stopband energy of the low-pass filter with a stopband edge $\tilde{\Omega}_s$. The constrained minimization of Φ_l can be accomplished by invoking a nonlinear optimization software package, such as the subroutines LCONF/DLCONF in the IMSL library [11]. However, the maximum number of linearly independent responses formed by a P-tap FIR filter is P. Therefore, we need to multiply the resultant $H(e^{j\tilde{\Omega}})$ by a simple all-pass filter, which does not change the magnitude response of $H(e^{j\tilde{\Omega}})$, but provides extra freedoms for the FIF design. The response of the new prototype filter is $\hat{H}(e^{j\tilde{\Omega}})$. Note the phase response of the all-pass filter should change smoothly, as a sharp change means more sampling in the design process and a larger value of M and J to keep a good frequency invariant response.

We then follow the steps in [6] and apply the transformation $\tilde{\Omega} = ((\Omega_2/\mu\Omega_1) - \sin\theta_i) \cdot \pi$ to $\hat{H}(e^{j\tilde{\Omega}})$ and obtain the desired response $R(\Omega_1, \Omega_2)$. In general $R(\Omega_1, \Omega_2)$ has infinite support in the time domain. For an approximation, we sample $R(\Omega_1, \Omega_2)$ within the range $\Omega_1 \in (-\pi; \pi]$ and $\Omega_2 \in (-\pi; \pi]$, whereby the number of samples for Ω_1 and Ω_2 should exceed J and M, respectively. Thereafter, an inverse DFT is performed on the sampled data. The resultant 2-D impulse responses are truncated directly or by applying an appropriate window function according to the numbers M and J. The resultant FIF will have the desired zero response at θ_s.

As an example, the response of an 18×18 FIF is shown in Fig. 5 over the band $\Omega \in [0.35\pi; 0.95\pi]$ with $\mu = 1$ and its main beam pointing to $\theta_i = -25^\circ$. It is derived from a five-tap low-pass filter multiplied by the all-pass filter $(0.6 + z^{-1})/(1 + 0.6z^{-1})$, which is also used in the FIF design in our simulations. The approximate frequency invariant property is clearly visible.

IV. Simulation Results

In our simulations, the proposed GSC with parameters $M = 18$ and $J = 24$ is compared to a standard GSC with $M = 18$ and $J = 15$. The blocking matrix of our proposed GSC is formed by 17 FIFs, which are derived by a five-tap FIR filter multiplied by an all-pass filter. One adaptive weight is used for each of the FIF outputs. The signal of interest impinges from broadside in the presence of spatially and spectrally uncorrelated noise of a signal to noise ratio of 20 dB. Six interfering signals from the angles of $-25^\circ, -45^\circ, -65^\circ, 20^\circ, 40^\circ$ and 60°, respectively, illuminate the array at a signal to interference ratio of -20 dB. Both the interfering signals and the signal of interest have a bandwidth of $[0.35\pi; 0.95\pi]$. We use a normalized LMS algorithm for adaptation [9]. The normalized stepsizes are 0.08 for our method and 0.24 for the standard GSC, which have been empirically chosen in order to achieve the same steady-state mean square residual error.

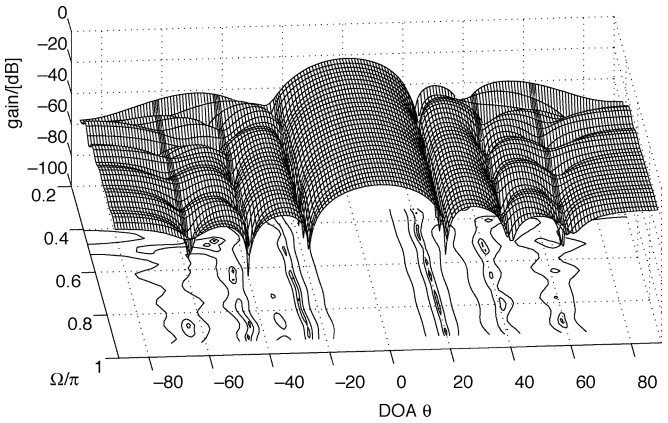

Fig. 7. 3-D beampattern of the proposed GSC over the bandwidth $\Omega \in [0.35\pi; 0.95\pi]$ and DOA range $\theta \in [-90^\circ; 90^\circ]$.

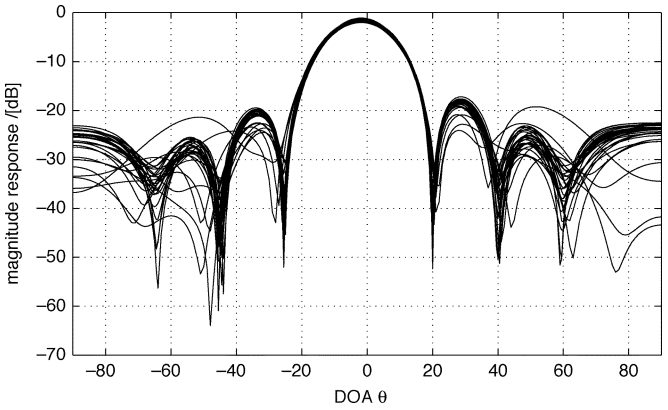

Fig. 8. 2-D beampattern of the proposed GSC over the bandwidth $\Omega \in [0.35\pi; 0.95\pi]$.

The learning curves of both methods are shown in Fig. 6. We see that even though for the standard GSC J is smaller and the stepsize is larger, the proposed method exhibits a considerably faster convergence due to the transformation effect of the FIFs and the resultant shorter adaptive filter length. In Fig. 7, we also provide the resultant beampattern of the proposed GSC over the bandwidth $\Omega \in [0.35\pi; 0.95\pi]$ and DOA range $\theta \in [-90^\circ; 90^\circ]$. The attenuation at the interferers' positions is clearly visible, and can be quantitatively inspected in Fig. 8, where the beamformer's response is shown over the band $\Omega = [0.35\pi; 0.95\pi]$.

Moreover, as the FIFs are approximately frequency invariant, the resultant 2-D and 3-D beampatterns will also be approximately frequency invariant, which can be verified from Figs. 7 and 8. To simply show the limitation of the beamspace method, in Fig. 6, we also give its learning curve with a stepsize of 0.01, where five FIFs are designed based on a five-tap FIR filter. As we have a total of seven signals, which is higher than the number of FIFs, the beamspace method in this case becomes incapable of reaching a low-level mean square residual error.

V. Conclusion

We have proposed a novel method for broadband adaptive beamforming based on the GSC structure, where the quiescent vector and blocking matrix are replaced by a series of 2-D FIFs. These FIFs transform the broadband beamforming problem into a narrowband one and ideally only one adaptive weight is required for each of the FIF outputs. Due to this transformation and the resultant low adaptive filter length, a considerably increased convergence speed is achieved, as demonstrated in our simulations.

References

[1] L. C. Godara, "Application of antenna arrays to mobile communications, part II: beam-forming and direction-of-arrival estimation," *Proc. IEEE*, vol. 85, no. 8, pp. 1195–1245, Aug. 1997.

[2] R. P. Gooch and J. J. Shynk, "Wide-band adaptive array processing using pole-zero digital filters," *IEEE Trans. Antennas Propag.*, vol. AP-34, no. 3, pp. 355–367, Mar. 1985.

[3] S. Weiss, R. W. Stewart, M. Schabert, I. K. Proudler, and M. W. Hoffman, "An efficient scheme for broadband adaptive beamforming," in *Asilomar Conference on Signals, Systems, and Computers*, vol. I, Monterey, CA, Nov. 1999, pp. 496–500.

[4] W. H. Neo and B. Farhang-Boroujeny, "Robust microphone arrays using subband adaptive filters," *Proc. Inst. Elect. Eng.—Vision, Image and Signal Processing*, vol. 149, no. 1, pp. 17–25, Feb. 2002.

[5] W. Liu, S. Weiss, and L. Hanzo, "A subband-selective broadband GSC with cosine-modulated blocking matrix," *IEEE Trans. Antennas Propag.*, vol. 52, no. 3, pp. 813–820, Mar. 2004.

[6] T. Sekiguchi and Y. Karasawa, "Wideband beamspace adaptive array utilizing FIR fan filters for multibeam forming," *IEEE Trans. Signal Processing*, vol. 48, no. 1, pp. 277–284, Jan. 2000.

[7] L. J. Griffiths and C. W. Jim, "An alternative approach to linearly constrained adaptive beamforming," *IEEE Trans. Antennas Propag.*, vol. 30, no. 1, pp. 27–34, Jan. 1982.

[8] O. L. Frost III, "An algorithm for linearly constrained adaptive array processing," *Proc. IEEE*, vol. 60, no. 8, pp. 926–935, Aug. 1972.

[9] S. Haykin, *Adaptive Filter Theory*, 3rd ed. Englewood Cliffs, NJ: Prentice-Hall, 1996.

[10] S. Haykin and J. Kesler, "Relation between the radiation pattern of an array and the two-dimensional discrete Fourier transform," *IEEE Trans. Antennas and Propagation*, vol. AP-23, no. 3, pp. 419–420, May 1975.

[11] Visual Numerics Inc., IMSL Fortran Numerical Libraries, San Ramon, CA, 2002.

An ADI-FDTD Method for Periodic Structures

Shumin Wang, Ji Chen, and Paul Ruchhoeft

***Abstract*—In this communication, the alternating-direction implicit finite-difference time-domain (ADI-FDTD) method is extended to analyze periodic structures. In the implicit updates of the ADI-FDTD method, the periodic boundary condition leads to a cyclic matrix. Instead of inverting the cyclic matrix directly, the problem is converted into two auxiliary linear systems that can be solved using the tridiagonal matrix solver. Consequently, only $7n$ arithmetic operations are required for each implicit update and the efficiency of the ADI-FDTD method is retained. Numerical examples further demonstrate the effectiveness of this periodic ADI-FDTD method.**

***Index Terms*—Alternating-direction implicit finite-difference time-domain (ADI-FDTD) method, periodic structure.**

I. Introduction

Periodic structures find many applications in engineering electromagnetics, such as filters, polarizers and radomes, etc. [1]. Because they are electrically large, numerical methods that incorporate the periodic characteristics are typically more appropriate. In these methods, instead of analyzing the entire structure, only a single-unit cell needs to be modeled. Among these techniques, the periodic finite-difference time-domain (FDTD) is an efficient algorithm derived from the conventional FDTD method [2], [3]. Besides the aforementioned advantages, the periodic FDTD method can easily handle material inhomogeneities. Furthermore, its solving procedure is more straightforward than other numerical methods, such as the method of moments (MoM) and the finite element method (FEM) [4].

Since the periodic FDTD method is derived from the conventional FDTD method, the time-step size of the periodic FDTD method cannot exceed the Courant–Friedrichs–Lewy (CFL) limitation [5]. This leads to computational inefficiency because fine meshes, which are often required to model large field variations and/or fine structures, would result in unwanted small time-step sizes. To circumvent this constraint, unconditionally stable FDTD algorithms become necessary. In particular, the alternating-direction implicit (ADI)-FDTD (ADI-FDTD) method is one of the promising numerical techniques that may improve the efficiency of the FDTD method for such applications [6]. In addition to its unconditional stability, the ADI-FDTD method generates tridiagonal matrices that can be solved with $O(n)$ operation count [7]. This is more advantageous than other unconditionally stable algorithms, because most of them require computationally expensive procedures to solve general sparse matrices.

In this paper we shall extend the ADI-FDTD method to analyze periodic structures in the case of two-dimensional (2-D) TE_z wave and normal incidence. Due to the periodic nature, cyclic matrices, instead of tridiagonal matrices, will be generated. Without care, the main advantage of the ADI-FDTD method may be lost. Here, we introduce a treatment by using the Sherman–Morrison formula. This treatment considers the aforementioned cyclic matrix as the perturbation of a general tri-diagonal matrix. The original problem of solving a linear system with a cyclic matrix is transformed into solving two auxiliary

Manuscript received July 16, 2004; revised January 13, 2005.

S. Wang is with Kelly Scientific, Incorporated, Bethesda, MD 20892 USA (e-mail: james.wang@ieee.org).

J. Chen and P. Ruchhoeft are with the Department of Electrical and Computer Engineering, University of Houston, Houston, TX 77204 USA.

Digital Object Identifier 10.1109/TAP.2005.850763